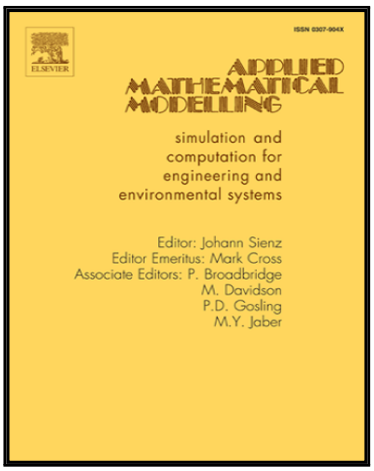


# A new hybrid uncertainty optimization method for structures using orthogonal series expansion

Jinglai Wu , Zhen Luo , Hao Li , Nong Zhang

PII: S0307-904X(17)30010-0
DOI: 10.1016/j.apm.2017.01.006
Reference: APM 11502

To appear in: *Applied Mathematical Modelling*

Received date: 11 May 2016
Revised date: 10 November 2016
Accepted date: 4 January 2017

Please cite this article as: Jinglai Wu , Zhen Luo , Hao Li , Nong Zhang , A new hybrid uncertainty optimization method for structures using orthogonal series expansion, *Applied Mathematical Modelling* (2017), doi: 10.1016/j.apm.2017.01.006

## Highlights:

- Proposal of a new uncertain structural optimization method under hybrid uncertainties;
- Design optimization formulated with the feasible robustness and reliability of the worst scenario;
- The hybrid uncertainty is quantified by using the orthogonal series expansion method;
- Polynomial Chaos (PC) expansion and Chebyshev interval methods integrated in a uniform framework;
- Design sensitivities developed to greatly facilitate the use of gradient-based optimization algorithms.

*Submitted to **Applied Mathematical Modelling**, Revised Submission: APM-D-16-01202R2*

# *A new hybrid uncertainty optimization method for structures using orthogonal series expansion*

by

**Jinglai Wu [1,2], Zhen Luo [1,*], Hao Li[1,2], Nong Zhang[1]**

[1] *School of Electrical, Mechanical and Mechatronic Systems*
*The University of Technology, Sydney, NSW 2007, Australia*

[2] *State Key Laboratory of Digital Manufacturing Equipment and Technology,*
*School of Mechanical Science and Engineering,*
*Huazhong University of Science and Technology, Wuhan, Hubei 430074, China*

Revised Submission (Version 2): *APM-D-16-01202R2*, 10 November, 2016

*Correspondence author in the process of manuscript submission
(Dr. Z. Luo, Email: zhen.luo@uts.edu.au, Tel: +61-2-9514-2994; Fax +61-2-9514-2655)

---

This paper is submitted for possible publication in ***Applied Mathematical Modelling***. It has not been previously published, is not currently submitted for review to any other journals, and will not be submitted elsewhere during the peer review.

---

**ABSTRACT**

This paper proposes a new hybrid uncertain design optimization method for structures which contain both random and interval variables simultaneously. The optimization model is formulated with the feasible robustness and the reliability of the worst scenario. The hybrid uncertainty is quantified by using the orthogonal series expansion method that integrates the Polynomial Chaos (PC) expansion method and the Chebyshev interval method within a uniform framework. The design sensitivity of objective and constraints will be developed to greatly facilitate the use of gradient-based optimization algorithms. The numerical results show that this method will be more possible to seek the feasible solution.

**Keywords:** hybrid uncertain optimization; orthogonal series expansion; Polynomial Chaos expansion; Chebyshev interval method.

## 1. Introduction

In engineering, the majority of research works for structural problems are based on the assumption that all parameters of the systems are deterministic. However, a number of real-world problems inherently contain numerous uncertain factors, e.g. various uncertainties are involved in loads, parameters, material properties, fraction tolerance, boundary conditions and geometric dimensions in the whole life cycle of design, manufacturing, service and aging. To enhance structural design performance and safety, there is an increasing demand to incorporate the impact of uncertainties quantitatively into the design problem of structures. In the area of uncertain optimization, the reliability-based design optimization (RBDO) and the robust design optimization (RDO) represent two major paradigms. RBDO [1] is a well-known type of design method under uncertainties, which has been widely studied over the past decades [2-6]. RBDO focuses on a risk-based solution taking into account the feasibility of target at expected probabilistic levels, in which the risk measure is commonly expressed by the probabilities of failure. Besides the RBDO, RDO [7] is another important type of design method consisting of uncertainties, which aims to determine a design to optimize the deterministic performance, while making it insensitive with respect to uncertain variables. As a matter of fact, the RBDO and RDO can be studied in a unified framework [7, 8], as the RBDO and RDO belong to the broad family of design optimization under uncertainty.

The implementation of the design optimization considering uncertain parameters generally contains two procedures. The first is the optimization algorithm for seeking the optimum solution at the nominal values of the design variables, while the second is the uncertainty quantification that quantifies the uncertainty by using some evaluation indexes, such as the probability of failure or the generalized reliability index [4], the variance of evaluation functions (objective and constraint functions) in RDO [9] and so on. In most

cases, the two procedures are implemented by using the double-loop [1, 10] or the sequential single-loop optimization [11]. There also have been some studies that try to combine the two procedures into one single step, e.g. the single-loop optimization in RBDO [3, 12, 13]. Since the first procedure only refers to the conventional optimization algorithms, the second procedure for uncertainty quantification (or uncertainty analysis) will be the key for design optimization under uncertainty.

Uncertainty can be classified into two different types [14, 15], namely aleatory and epistemic uncertainty. Aleatory uncertainty, also termed as objective or stochastic uncertainty, describes the inherent variation associated with a physical system or environment. Epistemic uncertainty or subjective uncertainty, on the other hand, derives from some level of ignorance or incomplete information about a physical system or environment. The aleatory uncertainty is commonly expressed by the random variables while the epistemic uncertainty may be described as the interval variables or fuzzy variables and so on. Since a number of engineering problems not only involve the aleatory uncertainty but also contain the epistemic uncertainty, this paper studies the design optimization problems of structures under the hybrid uncertainty.

In the quantification of the uncertainty about random variables, the optimization method [1], Monte Carlo simulation [16, 17], and Polynomial Chaos (PC) expansion method [18, 19] are usually employed. The optimization method is mainly used in the first-order reliability method (FORM) to find the most probable point (MPP) [3]. The optimization method has also been combined with the response surface method to quantify uncertainty [5, 20]. The Monte Carlo simulation can be conveniently implemented to produce a more comprehensive statistic information for evaluation functions, such as mean, variance, probability of failure, probability density function (PDF) and cumulative distribution function (CDF). However, the Monte Carlo simulation usually requires the information from a large number of sampling points. Its rate of convergence is of order $1/\sqrt{N}$ , which may be computationally prohibitive in engineering. The PC expansion method which is a kind of spectral decomposition method can be used to estimate the response of system with random variables, to greatly reduce the computational cost. The PC expansion method expands evaluation functions with respect to random variables using the corresponding orthogonal polynomials. After the PC expansion, the mean and variance of the evaluation functions can be calculated conveniently by using the characteristic of the orthogonal polynomials, and the Monte Carlo simulation may also be applied to estimate the PDF and CDF of the evaluation functions after the expansion. More application of the PC expansion method can be found in [21-25].

For interval uncertainty analysis, the evaluation indexes of uncertainty are described by the upper and lower bounds (maximum and minimum values) of the evaluation functions. The bounds of evaluation functions can be calculated using optimization methods [26, 27] or interval arithmetic [28-31]. The

optimization methods may capture the exact bounds of the evaluation functions if the optimization algorithms have the capacity to seek the global optimum. Since the global optimization algorithms are generally time-consuming, the gradient-based optimization algorithms are usually employed to find a local optimum solution, which will be effective when there are not multiple local optimal solutions in the uncertainty range. Interval arithmetic is the other effective method to estimate the bounds of the evaluation function, and it may produce an envelope of the evaluation function. The interval arithmetic has higher efficiency than the optimization algorithm, but the envelope is usually wider than the actual bounds, which is known as the overestimation phenomenon [32]. There have been some techniques developed to control the overestimation, such as the Taylor series expansion method [33, 34] and Chebyshev interval method [35]. The Chebyshev interval method expands the evaluation function with respect to the interval variables using the Chebyshev polynomials and then uses the interval arithmetic to estimate their bounds In fact, the Chebyshev method is also a special case of spectral decomposition method, since it expands the original function as an orthogonal series. However, the Chebyshev polynomials expansion only needs the information of bounds rather than the precise information of the probability distribution for uncertain variables, which is different from the traditional PC expansion for problems with random variables.

The uncertainty quantification methods mentioned above are only focused on one type of uncertainty, but many engineering problems involve both types of uncertainty simultaneously. Qiu et al. [36] proposed a probabilistic and interval hybrid reliability model to solve the structural design optimization problem, but the expression of limit state functions is required to be simple. Gao et al. [37] studied the hybrid uncertainty analysis for structures, in which both the Taylor expansion and Monte Carlo simulation are combined to determine the bounds of mean and standard deviation of the evaluation functions. Jiang et al. [38] employed the nested double-loop optimization to implement the analysis of hybrid uncertainty, in which the outer layer optimization is to find the MPP induced by the aleatory uncertainty and the inner layer optimization is to seek the extreme values under epistemic uncertainty. Li et al. [10] presented a multi-objective robust optimization to explore the design problems of parametric uncertainties involving both random and interval variables in foam filled thin-walled tube, in which the nested optimization procedure and Kriging surrogate model were employed.

The nested optimization is computationally prohibitive for structural design problems in engineering, so Du et al. [39] used the sequential single-loop optimization to analysis the hybrid uncertainty. Luo et al. [40] also proposed a sequential approximate programming and iteration scheme to solve the RBDO with hybrid uncertainties. Ge et al. [41] applied the single-loop optimization for the hybrid reliability assessment. A hybrid approach for the analysis of randomly vibrating structures was presented in

reference [42], in which the random process and fuzzy variables were used the describe the hybrid uncertainty. The optimization algorithm is used to handle the fuzzy variables. Eldred et al. [43] combined the PC expansion and interval optimization to quantify the hybrid uncertainty. However, most of the methods mentioned above are normally realized by using the optimization algorithms so that the efficiency will be low. Recently, Wu et al. [44] combined PC expansion method and Chebyshev interval method to develop a new uncertainty analysis method for vehicle dynamics performance under the hybrid uncertainty, which will be employed in this study.

In this paper, we will systematically combine the interval arithmetic, the Monte Carlo simulation and the PC expansion theory to quantify the hybrid uncertainty, so as to deliver a new hybrid uncertainty based optimization method for structures including design sensitivity analysis for interval mean and interval standard deviation. In the proposed method, the evaluation functions are firstly expanded via a series of orthogonal polynomials with respect to both the random and interval variables. After the expansion, the interval mean and interval variance of evaluation functions are calculated conveniently and effectively by using the characteristic of orthogonal polynomials. At the same time, the derivatives of the interval objective function and constraints can be evaluated, to enable the application of gradient-based optimization algorithms to the uncertainty design optimization. Finally, the Monte Carlo simulation will be applied to estimate the PDF and CDF of the two bounds of the evaluation functions. It is noted that the Monte Carlo simulation is not computationally expensive in this case, because we have built a relatively cheap (orthogonal series based) surrogate model for the original complicated evaluation functions. The optimization under hybrid uncertainty is formulated with the feasible robustness under the aleatory uncertainty and the reliability of the worst scenario under the epistemic uncertainty. Two typical numerical examples will be used to demonstrate the effectiveness of the proposed method.

## 2. Hybrid uncertainty optimization model

The conventional deterministic optimization model can be expressed as follows:

$$\begin{cases} \min\limits_{\mathbf{x}} & f(\mathbf{x}) \\ \text{s.t.} & \mathbf{g}(\mathbf{x}) \le \mathbf{0} \\ & \mathbf{x}^l \le \mathbf{x} \le \mathbf{x}^u \end{cases} \tag{1}$$

where $\mathbf{x} \in R^m$ are the $m$-dimensional design variables, $f(\mathbf{x})$ is the objective function, and $\mathbf{g}(\mathbf{x}) = [g_1(\mathbf{x}) \quad \cdots \quad g_k(\mathbf{x})]^{\mathrm{T}}$ is the $k$-dimensional constraints. All the design variables in the vector $\mathbf{x}$ and other parameters are deterministic in the above equation.

As aforementioned, we will extend the deterministic optimization problem as an uncertain optimization problem. If the design variables and parameters are supposed to involve uncertainty, there may be some

uncertain variables contained in both objective and constraint functions. Thus, the optimization formulation will be changed to the following model

$$\begin{cases} \min\limits_{\mathbf{x}} & f(\mathbf{x}+\boldsymbol{\eta},\boldsymbol{\xi}) \\ \text{s.t.} & \mathbf{g}(\mathbf{x}+\boldsymbol{\eta},\boldsymbol{\xi}) \le \mathbf{0} \\ & \mathbf{x}^l \le \mathbf{x} \le \mathbf{x}^u \end{cases} \tag{2}$$

where $\boldsymbol{\eta}=[\eta_1 \ \ldots \eta_m]^{\mathrm{T}}$ are the uncertain part of the design variables, $\boldsymbol{\xi}=[\xi_1 \ \ldots \ \xi_n]^{\mathrm{T}}$ denotes the uncertain parameters. It is noted that the $\boldsymbol{\eta}$ and $\boldsymbol{\xi}$ can be either random variables or interval variables, or the mixture of random and interval variables. However, for simplicity but without losing any generality, this study will only consider parameters $\boldsymbol{\xi}$ as the $n$-dimensional independent random variables, and $\boldsymbol{\eta}$ as the $m$-dimensional independent interval variables, to be noted by $[\boldsymbol{\eta}]=[\underline{\boldsymbol{\eta}},\overline{\boldsymbol{\eta}}]$, in which $\underline{\boldsymbol{\eta}}$ and $\overline{\boldsymbol{\eta}}$ are the lower bounds and upper bounds of the interval variables, respectively.

Since both the objective function $f$ and constraints $\mathbf{g}$ contain the uncertain variables, the objective and constraints should be re-formulated to reflect the influence of the uncertainty. Firstly, if only the random variables are included in $f$ and $\mathbf{g}$, the mean $\mu_f$ and $\boldsymbol{\mu}_{\mathbf{g}}$, as well as the variance $\sigma_f^2$ and $\boldsymbol{\sigma}_{\mathbf{g}}^2$ are usually used as uncertainty evaluation indexes. For the feasible robustness approach, the objective and constraints will be the weighted summation of the mean value and standard deviation, so the uncertain optimization model can be transformed to the following expression [7, 45, 46]

$$\begin{cases} \min\limits_{\mathbf{x}} & w_1\mu_f\left(\mathbf{x}+[\boldsymbol{\eta}],\boldsymbol{\xi}\right)+w_2\sigma_f\left(\mathbf{x}+[\boldsymbol{\eta}],\boldsymbol{\xi}\right) \\ \text{s.t.} & w_3\boldsymbol{\mu}_{\mathbf{g}}\left(\mathbf{x}+[\boldsymbol{\eta}],\boldsymbol{\xi}\right)+w_4\boldsymbol{\sigma}_{\mathbf{g}}\left(\mathbf{x}+[\boldsymbol{\eta}],\boldsymbol{\xi}\right) \le \mathbf{0} \\ & \mathbf{x}^l \le \mathbf{x} \le \mathbf{x}^u \end{cases} \tag{3}$$

where $w_1$ and $w_2$ are the weighting coefficients for the mean value and standard deviation in the objective function. Here we can set them as $w_1 = 1$, and $w_2 = 1$. It is noted that there is no requirement that $w_1 + w_2 = 1$, as the value of an objective function can be multiplied by a positive number, which does not change the characteristics of the original objective function in the optimization process. In this case, the optimization under the new objective function will provide the same optimal point as the original objective function. $w_3$ and $w_4$ are also the weighting coefficients for the mean and standard deviation of the constraints, and set as $w_3 = 1$, and $w_4 = 3$ in this paper. If the constraints can approximately satisfy the normal distribution, the probability is given by $\Phi(w_4)$, where $\Phi$ is the cumulative distribution function of a standard normal variable. For example, in this paper $w_4$ is considered as 3 which means that the probability of the constraint satisfaction will be $\Phi(3)=0.9987$ [45]. Fig. 1 is used to express the constraints in the RDO. If the constraints are close to the normal distribution, the solution (red solid line) obtained by using the constraint of RDO model has quite small probability to fail, but solution (blue dash line) of the deterministic optimization model has almost 50% probability to fail.

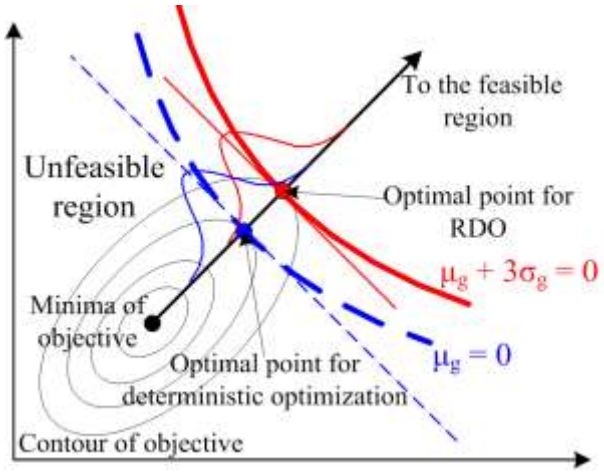


Figure 1 Constraints of RDO

For the stochastic optimization problem, there are several types of RDO models considering random variables, depending on the expressions for robustness measures, which mainly contain the expectance measure of robustness which is used in this paper, probabilistic threshold measure of the robustness, and statistical feasibility robustness [45]. In general, the expectance measure can be obtained more easily than the other two measures, because the expectance measure only depends on the mean and variance while other two measures compute the conditional CDF of the objective or constraint functions. This paper uses the expectance measure, as the PC expansion can obtain the mean and variance convinently. It is worth to note that the PC expansion can also be used to compute the CDF, but an additional Monte Carlo simulation may be required after the implementation of PC expansion, which costs the computation in the optimization process.

Secondly, considering the additional interval uncertainty [$\boldsymbol{\eta}$] included in the Eq. (3), the value of the mean and standard deviation would also be an interval number rather than a real number. Therefore, the mean and standard deviation vary between their lower bounds and upper bounds. To guarantee the reliability, the worst case scenario will be considered in the optimization formulation, which uses the maximum value (or the upper bounds) of the original objective function and constraints as the new objective function and constraints. Hence, the optimization model can be expressed as follows:

$$\begin{cases} \min\limits_{\mathbf{x}} & w_1\bar{\mu}_f\left(\mathbf{x}+[\boldsymbol{\eta}],\boldsymbol{\xi}\right)+w_2\bar{\sigma}_f\left(\mathbf{x}+[\boldsymbol{\eta}],\boldsymbol{\xi}\right) \\ \text{s.t.} & \bar{\boldsymbol{\mu}}_{\mathbf{g}}\left(\mathbf{x}+[\boldsymbol{\eta}],\boldsymbol{\xi}\right)+w_3\bar{\boldsymbol{\sigma}}_{\mathbf{g}}\left(\mathbf{x}+[\boldsymbol{\eta}],\boldsymbol{\xi}\right)\le\mathbf{0} \\ & \mathbf{x}^l\le\mathbf{x}\le\mathbf{x}^u \end{cases} \tag{4}$$

The above optimization problem can be solved by many traditional optimization methods. Here the discussion of the optimization algorithm is out of the major scope of this study. The key procedure in the optimization is the evaluation of the objective function and constraints. Both the objective function and

constraints are composed of the bounds of interval mean and interval deviation, so how to obtain the two measure metrics efficiently is an important issue, which will be discussed in the next section.

## 3. Hybrid uncertainty analysis method

### 3.1 Hybrid uncertainty analysis by the orthogonal series expansion

This section will briefly discuss the orthogonal series expansion (OSE) method for analysis of the hybrid uncertainty. For more details readers can be referred to [44]. Consider the function $F(\boldsymbol{\xi}, [\boldsymbol{\eta}])$ which includes both the random variables $\boldsymbol{\xi}$ and interval variables $[\boldsymbol{\eta}]$, where the $n$-dimensional random variables are assumed to be in the form of standard Gaussian distribution $\boldsymbol{\xi} \in N(0, 1)^n$ and the $m$-dimensional interval variables are defined as $[\boldsymbol{\eta}]=[-1, 1]^m$.

To evaluate the interval mean and interval variance of $F(\boldsymbol{\xi}, [\boldsymbol{\eta}])$, which will be expanded by using the $p$-th order of truncated sparse Hermite series with respect to the random variables $\boldsymbol{\xi}$ as

$$F(\boldsymbol{\xi},[\boldsymbol{\eta}]) = \sum_{j=0}^{S-1} \beta_j([\boldsymbol{\eta}])\phi_j(\boldsymbol{\xi}) \tag{5}$$

where the $\beta_j([\boldsymbol{\eta}])$ denotes the coefficients of Hermite polynomials, $\phi_j$ denotes the $n$-dimensional sparse Hermite polynomials which are the basis of the expansion and are produced by the product of 1-dimensional Hermite polynomials, shown as

$$\begin{aligned}
&\phi_0(\boldsymbol{\xi}) = 1,\\
&\phi_1(\boldsymbol{\xi}) = H_1(\xi_1),\ \ldots,\phi_n(\boldsymbol{\xi}) = H_1(\xi_2),\\
&\phi_{n+1}(\boldsymbol{\xi}) = H_2(\xi_1),\phi_{n+2}(\boldsymbol{\xi}) = H_1(\xi_1)H_1(\xi_2),\ \ldots,P_{\frac{(n+2)!}{2!n!}-1}(\boldsymbol{\xi}) = H_2(\xi_n),\\
&\ldots
\end{aligned} \tag{6}$$

where $H_i$ denotes the 1-dimensional Hermite polynomial with order $i$. $S$ is the number of terms of the $n$-dimensional sparse Hermite series with order $p$, i.e. $S=(n+p)!/(n!p!)$. The Hermite polynomials for functions with Gaussian random variables can get the optimal convergence. For the random variable with uniform probability distribution, the Legendre polynomials are used as the basis that can produce better accuracy. More orthogonal polynomials basis for other random variables can be found in [19].

The coefficients $\beta_j([\boldsymbol{\eta}])$ have a relationship with interval variables $[\boldsymbol{\eta}]$, so they can be expanded by the Chebyshev polynomials [35]. Expanding the coefficients $\beta_j([\boldsymbol{\eta}])$ with respect to $[\boldsymbol{\eta}]$ using the $p$-th order truncated Chebyshev series, we can obtain its Chebyshev inclusion function as follows:

$$[\beta_j]([\boldsymbol{\eta}])=\sum_{i=0}^{K-1} \beta_{i,j}\psi_i([\boldsymbol{\eta}]) \tag{7}$$

Here $\beta_{i,j}$ denotes the elements in the coefficient matrix $\boldsymbol{\beta}$ with $K$ rows and $S$ columns, $\psi_i$ denotes the $m$-dimensional sparse Chebyshev polynomials [35, 44], and $K$ is number of terms of $m$ dimensional Chebyshev series with order $p$, i.e. $K=(m+p)!/(m!p!)$.

The coefficient matrix $\boldsymbol{\beta}$ can be obtained by using the least squares method twice [44]

$$\boldsymbol{\beta}=\left(\mathbf{X}_1(\boldsymbol{\eta})^{\mathrm{T}}\mathbf{X}_1(\boldsymbol{\eta})\right)^{-1}\mathbf{X}_1(\boldsymbol{\eta})^{\mathrm{T}}\mathbf{F}^{\mathrm{T}}\mathbf{X}_2(\boldsymbol{\xi})\left(\mathbf{X}_2(\boldsymbol{\xi})\mathbf{X}_2(\boldsymbol{\xi})^{\mathrm{T}}\right)^{-1} \tag{8}$$

where $\mathbf{X}_1$ is the transform matrix about the interval variables, $\mathbf{X}_2$ is the transform matrix about random variables, and $\mathbf{F}$ is the function value matrix at the collocation points of random variables and interval variables. Using $\boldsymbol{\Phi}=[\phi_0,\ \cdots,\ \phi_{S-1}]^{\mathrm{T}}$ and $\boldsymbol{\Psi}=[\psi_0,\ \cdots,\ \psi_{K-1}]^{\mathrm{T}}$ to denote the vectors of Hermite polynomials and Chebyshev polynomials, respectively, the two transform matrix will be expressed by

$$\mathbf{X}_1(\boldsymbol{\eta})=\left[\boldsymbol{\Psi}(\boldsymbol{\eta}^{(1)})\quad\cdots\quad\boldsymbol{\Psi}(\boldsymbol{\eta}^{(M)})\right]^{\mathrm{T}},\ \mathbf{X}_2(\boldsymbol{\xi})=\left[\boldsymbol{\Phi}(\boldsymbol{\xi}^{(1)})\quad\cdots\quad\boldsymbol{\Phi}(\boldsymbol{\xi}^{(N)})\right]^{\mathrm{T}} \tag{9}$$

where the $\boldsymbol{\xi}^{(i)}(i=1,...,N)$ denotes the collocation points of the random variables which are selected from the zeros of Hermite polynomials with order $p$+1, and $\boldsymbol{\eta}^{(i)}$ ($i=1,...,M$) are the collocation points of interval variables selected from the zeros of the ($p$+1)-th Chebyshev polynomials [35, 44]. To enhance the numerical stability of the least squares method in Eq. (8), the number of collocation points are usually selected by the following criteria: $N\geq 2S$ and $M\geq 2M$. Hence, the matrix of function value is expressed as

$$\mathbf{F}=\begin{bmatrix} F(\boldsymbol{\xi}^{(1)},\boldsymbol{\eta}^{(1)}) & \cdots & F(\boldsymbol{\xi}^{(1)},\boldsymbol{\eta}^{(M)}) \\ \vdots & \ddots & \vdots \\ F(\boldsymbol{\xi}^{(N)},\boldsymbol{\eta}^{(1)}) & \cdots & F(\boldsymbol{\xi}^{(N)},\boldsymbol{\eta}^{(M)}) \end{bmatrix} \tag{10}$$

The order $p$ for the expansion process can be determined by the variation of coefficients $\boldsymbol{\beta}$. In general physical problems, the low-order terms dominate the system rather than the high-order terms, which means the coefficients of high-order terms will be convergent to 0 gradually. Therefore, we can increase the order of the orthogonal series sequentially and compare the variation of coefficients to determine the order to be used. The termination criterion can be defined as following expression

$$\frac{\left|\sum\left\|\boldsymbol{\beta}_{p+1}\right\|_1-\sum\left\|\boldsymbol{\beta}_{p}\right\|_1\right|}{\sum\left\|\boldsymbol{\beta}_{p}\right\|_1}\leq c \tag{11}$$

where the subscript $p$ denotes the order of the expansion, and $c$ is a small criterion number, e.g. $c$=2% used in this paper. Once the previous criterion is satisfied, we can stop to increase the order of expansion and use the $p$-th order orthogonal series to expand the original function.

The Chebyshev series may be transformed to the power series, so the Eq. (7) can be expressed by the following power series

$$[\beta_j]([\boldsymbol{\eta}])=\sum_{i=0}^{K-1}\beta_{i,j}\psi_i([\boldsymbol{\eta}])=\sum_{i=0}^{K-1}\alpha_{i,j}P_i([\boldsymbol{\eta}]) \tag{12}$$

where $\alpha_{i,j}$ are the elements of coefficient matrix $\boldsymbol{\alpha}$ of the power function $P_i$, and the $m$-dimensional power function $P_i(\boldsymbol{\eta})$ are defined as follows:

$$\begin{aligned}
&P_0(\boldsymbol{\eta})=1,\\
&P_1(\boldsymbol{\eta})=\eta_1,\ \ldots,P_m(\boldsymbol{\eta})=\eta_m,\\
&P_{m+1}(\boldsymbol{\eta})=\eta_1^2,P_{m+2}(\boldsymbol{\eta})=\eta_1\eta_2,\ \ldots,P_{\frac{(m+2)!}{2!m!}-1}(\boldsymbol{\eta})=\eta_m^2,\\
&\ldots
\end{aligned} \tag{13}$$

The coefficient matrix $\boldsymbol{\alpha}$ can be calculated by using a linear transformation from the coefficient matrix $\boldsymbol{\beta}$, or evaluated by the least squares method, i.e.

$$\boldsymbol{\alpha}=\left(\mathbf{X}_3(\boldsymbol{\eta})^{\mathrm{T}}\mathbf{X}_3(\boldsymbol{\eta})\right)^{-1}\mathbf{X}_3(\boldsymbol{\eta})^{\mathrm{T}}\mathbf{F}^{\mathrm{T}}\mathbf{X}_2(\boldsymbol{\xi})\left(\mathbf{X}_2(\boldsymbol{\xi})\mathbf{X}_2(\boldsymbol{\xi})^{\mathrm{T}}\right)^{-1} \tag{14}$$

where the $\mathbf{F}$ and $\mathbf{X}_2$ are as the same shown in Eqs. (9-10), and the transform matrix $\mathbf{X}_3$ is expressed by

$$\mathbf{X}_3(\boldsymbol{\eta})=\left[\mathbf{P}(\boldsymbol{\eta}^{(1)})\quad\cdots\quad\mathbf{P}(\boldsymbol{\eta}^{(M)})\right]^{\mathrm{T}} \tag{15}$$

Here $\mathbf{P}=[P_0,\ \cdots,P_{K-1}]^{\mathrm{T}}$ denotes the vector of the power function.

Once the coefficients are obtained, the interval mean $[\mu_F]$ and interval variance $[\sigma_F^2]$ of the evaluation functions can be calculated based on the PC expansion theory [18, 19] and interval arithmetic, as follows

$$[\mu_F]=[\beta_0]([\boldsymbol{\eta}])=\sum_{i=0}^{K-1}\alpha_{i,0}P_i([\boldsymbol{\eta}]) \tag{16}$$

$$[\sigma_F^2]=\sum_{j=1}^{S-1}[\beta_j]^2\left\langle\phi_j^2\right\rangle=\sum_{j=1}^{S-1}\left(\sum_{i=0}^{K-1}\alpha_{i,j}P_i([\boldsymbol{\eta}])\right)^2\left\langle\phi_j^2\right\rangle \tag{17}$$

where $<\phi_j^2>=<\phi_j,\phi_j>$ and the operation $<u, v>$ represents the inner product of $u$ and $v$.

Using Eqs. (16-17) to calculate the interval mean and interval variance of function $f$ and $\mathbf{g}$ given in Eq. (4), the uncertainty optimization can be implemented. It can be found that the proposed method handles the random variables and interval variables in one integrated framework, and can be implemented easily. After obtain the function value matrix $\mathbf{F}$ at the collocation points (Eq. (10)), the coefficients can be produced by the least squares method, and then the interval mean and variance can be calculated according to the above two equations.

### 3.2 Sensitivity analysis with the hybrid uncertainty

When the gradient-based optimization algorithms are used as the optimization algorithm, the derivatives of objective and constraints with respect to the design variables are required. Although the finite difference method can be used to approximate the derivatives, the computational cost will be expensive so the numerical accuracy will be low for large-scale optimization problems. In this section, we will derive the first-order derivatives of the interval mean and interval standard deviation.

Based on Eq. (4), it can be found that the derivatives of the evaluation functions (both the objective function and the constraints functions) with respect to **x** is equal to the derivatives with respect to **η**, Considering the 1-dimensional case, the coefficients of Hermite polynomials in Eq. (12) can be regarded as a standard power series with respect to $[\eta]$

$$[\beta_j]([\eta]) = \sum_{i=0}^{K-1} \alpha_{i,j} P_i([\eta]) = \alpha_{0,j} + \sum_{i=1}^{K-1} \alpha_{i,j} [\eta]^i \tag{18}$$

If there is a small increment $\Delta\eta$, the coefficient can also be expressed as another standard power series

$$[\beta_j]([\eta]+\Delta\eta) = \alpha_{0,j} + \sum_{i=1}^{k-1} \alpha_{i,j} \left([\eta]+\Delta\eta\right)^i = b_{0,j} + \sum_{i=1}^{k-1} b_{i,j} [\eta]^i \tag{19}$$

where the coefficients $b_i$ will be determined by

$$b_{i,j} = \alpha_{i,j} + (i+1)\alpha_{i+1,j}\Delta\eta + \mathrm{O}\left(\Delta\eta^2\right) \tag{20}$$

Using the interval arithmetic, the upper and lower bound of the coefficients can be calculated by

$$\overline{\beta}_j = \alpha_{0,j} + \sum_{i=2q-1} \alpha_{i,j} \mathrm{sign}\left(\alpha_{i,j}\right) + \sum_{i=2q} \alpha_{i,j} H\left(\alpha_{i,j}\right) \tag{21}$$

$$\underline{\beta}_j = \alpha_{0,j} + \sum_{i=2q-1} \alpha_{i,j} \mathrm{sign}\left(-\alpha_{i,j}\right) + \sum_{i=2q} \alpha_{i,j} H\left(-\alpha_{i,j}\right) \tag{22}$$

where $q$ denotes the positive integer, and the sign function sign($x$) and Heaviside step function $H(x)$ are defined as

$$\mathrm{sign}(x) = \begin{cases} 1, & x > 0 \\ -1, & x \le 0 \end{cases}, \quad H(x) = \begin{cases} 1, & x > 0 \\ 0, & x \le 0 \end{cases} \tag{23}$$

Combining Eqs. (18)-(22) and neglecting the discontinuous points that are $\alpha_{i,j}$ =0, the derivative of the two bounds of the coefficients can be expressed by

$$\frac{\partial \overline{\beta}_j}{\partial \eta} = \lim_{\Delta\eta\to 0} \frac{\overline{\beta}_j([\eta]+\Delta\eta) - \overline{\beta}_j([\eta])}{\Delta\eta} = \alpha_{1,j} + \sum_{i=2q-1} (i+1)\alpha_{i+1,j} \mathrm{sign}\left(\alpha_{i,j}\right) + \sum_{i=2q} (i+1)\alpha_{i+1,j} H\left(\alpha_{i,j}\right) \tag{24}$$

$$\frac{\partial \underline{\beta}_j}{\partial \eta} = \lim_{\Delta\eta\to 0} \frac{\underline{\beta}_j([\eta]+\Delta\eta) - \underline{\beta}_j([\eta])}{\Delta\eta} = \alpha_{1,j} + \sum_{i=2q-1} (i+1)\alpha_{i+1,j} \mathrm{sign}\left(-\alpha_{i,j}\right) + \sum_{i=2q} (i+1)\alpha_{i+1,j} H\left(-\alpha_{i,j}\right) \tag{25}$$

The Eqs. (24-25) contain the sign function and Heaviside step function, which will make the derivatives unsmooth. The unsmooth derivatives may make the optimization process unstable, so the following approximation projection method is used to smooth the sign function and Heaviside step function

$$\operatorname{sign}(x) \approx \tanh(\gamma x),\ H(x) \approx \frac{1}{2} + \frac{1}{2}\tanh(\gamma x) \tag{26}$$

where the coefficient γ is a positive real number. The function tanh(γ*x*) will be equal to sign(*x*) when the parameter γ tends to be infinite. Therefore, the derivatives of the two bounds will be transformed to

$$\frac{\partial \overline{\beta}_j}{\partial \eta} = \alpha_{1,j} + \sum_{i=2q-1} (i+1)\alpha_{i+1,j}\tanh\left(\gamma\alpha_{i,j}\right) + \sum_{i=2q} \frac{i+1}{2}\alpha_{i+1,j}\left(1+\tanh\left(\gamma\alpha_{i,j}\right)\right) \tag{27}$$

$$\frac{\partial \underline{\beta}_j}{\partial \eta} = \alpha_{1,j} + \sum_{i=2q-1} (i+1)\alpha_{i+1,j}\tanh\left(-\gamma\alpha_{i,j}\right) + \sum_{i=2q} \frac{i+1}{2}\alpha_{i+1,j}\left(1+\tanh\left(-\gamma\alpha_{i,j}\right)\right) \tag{28}$$

Combining Eqs. (16) and (27), the derivative of the upper bound of the interval mean will be

$$\frac{\partial \overline{\mu}_F}{\partial \eta} = \frac{\partial \overline{\beta}_0}{\partial \eta} = \alpha_{1,0} + \sum_{i=2q-1} (i+1)\alpha_{i+1,0}\tanh\left(\gamma\alpha_{i,0}\right) + \sum_{i=2q} \frac{i+1}{2}\alpha_{i+1,0}\left(1+\tanh\left(\gamma\alpha_{i,0}\right)\right) \tag{29}$$

Using the interval arithmetic in Eq. (17), the upper bound of the interval variance can be calculated by

$$\overline{\sigma}_F^2 = \sum_{j=1}^{S-1} \max\left(\underline{\beta}_j^2, \overline{\beta}_j^2\right)\left\langle \phi_j^2 \right\rangle \tag{30}$$

Therefore, the derivative of the upper bound of the standard deviation is given as

$$\frac{\partial \overline{\sigma}_F}{\partial \eta} = \frac{1}{2\overline{\sigma}_F}\sum_{j=1}^{S-1} \frac{\partial\left(\max\left(\underline{\beta}_j^2, \overline{\beta}_j^2\right)\right)}{\partial \eta}\left\langle \phi_j^2 \right\rangle,\ \text{where}\ \frac{\partial\left(\max\left(\underline{\beta}_j^2, \overline{\beta}_j^2\right)\right)}{\partial \eta} = \begin{cases} 2\overline{\beta}_j \dfrac{\partial \overline{\beta}_j}{\partial \eta}, & \left|\overline{\beta}_j\right| \geq \left|\underline{\beta}_j\right| \\ 2\underline{\beta}_j \dfrac{\partial \underline{\beta}_j}{\partial \eta}, & \left|\overline{\beta}_j\right| < \left|\underline{\beta}_j\right| \end{cases} \tag{31}$$

Based on the sensitivity information given by Eq. (29) and (31), the hybrid uncertainty optimization defined in Eq. (4) can be implemented by conventional gradient-based optimization algorithms.

## 4. Quantification of hybrid uncertainty

We can obtain the interval mean and interval variance of evaluation functions based on the derivation in the previous section, but these two evaluation indexes may not provide the comprehensive information of the hybrid uncertainty. Besides the interval mean and interval variance, the hybrid uncertainty can be more comprehensively assessed by the p-box, the measures of belief and plausibility in the evidence theory [14, 47]. Here the PDF and CDF of the lower and upper bounds of evaluation functions will be applied to express the comprehensive information. The CDF of lower bound may be equivalent to the measure of belief, while the CDF of the upper bound may be equivalent to the measure of plausibility.

Substituting Eq. (7) into Eq. (5), the evaluation function can be expressed by

$$F\left(\boldsymbol{\xi},[\boldsymbol{\eta}]\right)=\sum_{j=0}^{S-1}\left(\sum_{i=0}^{K-1}\beta_{i,j}\psi_i\left([\boldsymbol{\eta}]\right)\right)\phi_j\left(\boldsymbol{\xi}\right)=\sum_{i=0}^{K-1}\left(\sum_{j=0}^{S-1}\beta_{i,j}\phi_j\left(\boldsymbol{\xi}\right)\right)\psi_i\left([\boldsymbol{\eta}]\right) \tag{32}$$

Therefore, the two bounds of the evaluation functions will be defined as

$$\underline{F}\left(\boldsymbol{\xi},[\boldsymbol{\eta}]\right)=\min_{\boldsymbol{\eta}}\sum_{i=0}^{K-1}\left(\sum_{j=0}^{S-1}\beta_{i,j}\phi_j\left(\boldsymbol{\xi}\right)\right)\psi_i\left(\boldsymbol{\eta}\right),\ \bar{F}\left(\boldsymbol{\xi},[\boldsymbol{\eta}]\right)=\max_{\boldsymbol{\eta}}\sum_{i=0}^{K-1}\left(\sum_{j=0}^{S-1}\beta_{i,j}\phi_j\left(\boldsymbol{\xi}\right)\right)\psi_i\left(\boldsymbol{\eta}\right) \tag{33}$$

The optimization algorithms or scanning method can be used to calculate the two bounds with respect to interval variables. On the other hand, the bounds of evaluation functions contain the random variables $\boldsymbol{\xi}$, so we can obtain the PDF and CDF of the bounds through the Monte Carlo simulation. It should be noted that both the optimization process and Monte Carlo simulation are not computationally expensive in this case, because the analytical expression (Eq. (32)) has been obtained.

To verify the proposed method, we consider the following test example. For simplicity, the $F(\xi,[\eta])$ is a scalar function containing 1-dimensional random variable $\xi\in N(0,\ 1)$ and 1-dimensional interval variable $[\eta]$=[-1, 1], which is defined as

$$F(\xi,[\eta])=\xi^2\sin\left(\frac{[\eta]}{2}\right) \tag{34}$$

The proposed orthogonal series is used to expand Eq. (34). Using the different order of polynomials to expand the function and computing the coefficients, we have $\sum\|\boldsymbol{\beta}_1\|_1=0.49,\sum\|\boldsymbol{\beta}_2\|_1=0.97$ , and $\sum\|\boldsymbol{\beta}_3\|_1=0.98$. Since the variation between the coefficient of the second order polynomial and third polynomial is very small, we will choose the second order polynomial to implement the OSE based on the Eq. (11). Therefore, the number of collocation points and interpolation points are set as $N$=$M$=3. As a result, the total number of computing points for the original function is $N\times M$=9.

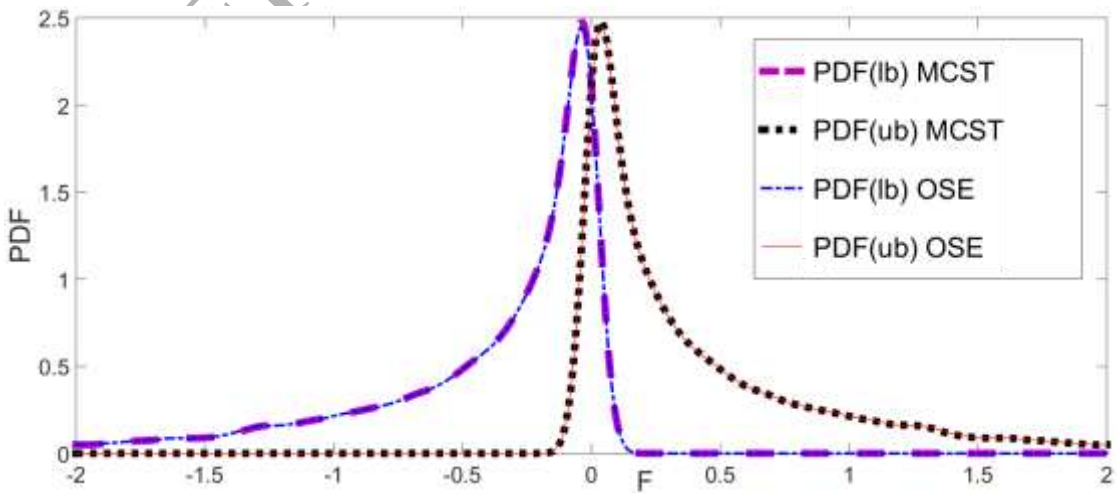


Figure.2 (a) The PDF of two bounds

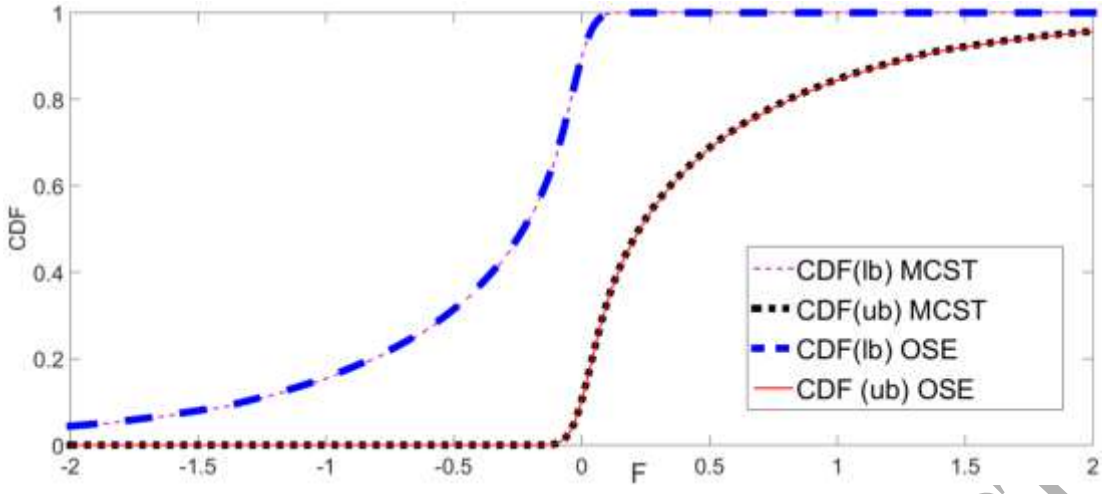


Figure.2 (b) The CDF of two bounds

("lb": lower bound; "ub": upper bound; "MCST": Monte-Carlo-Scanning-Test; "OSE": Orthogonal Series Expansion)

After obtaining the coefficients, the Monte Carlo simulation and optimization algorithm can be used to obtain the sampling data of the bounds. Based on a large amount of sampling data, we can plot the PDF and CDF of the two bounds for the function *F*, shown in Fig.2.

The reference result of the PDF and CDF of the two bounds can be obtained by the combination of Monte Carlo simulation and the scanning test for the original function, termed as Monte-Carlo-Scanning-Test (MCST). The MCST uses the Monte Carlo simulation collect the sampling points in the space of random variables and employs the scanning test that is a symmetrical dense grid to sample the space of interval variables. The scanning test will find the bounds of the evaluation function, and the Monte Carlo simulation will find the corresponding PDF and CDF. The results of MCST are also given in Fig.1, which shows that the PDF and CDF of two bounds obtained by the OSE method is very close to that of MCST. In practical applications, the cost of evaluating the original function is very expensive usually, so we use the number of evaluating the original function as the index of efficiency. For this numerical testing example, the 10000 samples are used in the Monte Carlo simulation and 10 symmetrical samples are used in the scanning test, so the total number computing the original function is 10000×10, which is much larger than the 9 samples used in the OSE method. Hence, the OSE method has higher efficiency than the MCST.

To demonstrate the efficiency of the proposed OSE method, another uncertain quantification method by Eldred et al. [43] was also employed in this paper in the test example. Eldred's method applied an optimization algorithm to seek the bounds of interval variables, and the PC expansion to handle random variables, so this method was a kind of interval optimization-based method. In ordedr to compare

Eldred's method with our OSE method, we still employ the second order polynomials expansion to handle the random variable, so the numbers of computing original functions for both methods are the same, namely 3. Here, the sequential quadratic programming (SQP) is used to find the bounds of the interval variable, and the two bounds are obtained after 16 evaluations of the original function. Since the function is monotonic with respect to the interval variable, the results obtained by the SQP method is globally optimal. As a result, the accuracy of the Eldred's interval optimization-based method is almost the same as the OSE method in this paper. However, the total number of function evaluations for Eldred's method is 16×3=48, which is also larger than the 9 samples used in the OSE method. Hence the proposed OSE method has higher efficiency than Eldred's method.

If the random variable is considered as constant, e.g. $\xi$=1, then CDF of the two bounds will be a degenerated into two vertical lines (pure interval), and the PDF will be infinite. On the other hand, if there is no interval variable in the function, the CDF of the two bounds will be one traditional CDF. Some researchers just consider the uncertain-but-bounded variables as uniformly distributed random variables, which may produce some large deviations. For example, if the uncertain variable $\eta$ in Eq. (34) is assumed to satisfy the uniform distribution, i.e. $\eta \sim$ U(-1,1), we can draw its PDF and CDF of $F(\xi, \eta)$ by using the Monte Carlo method, shown in Fig. 3. However, if the actual probability distribution is $\eta \sim$ Beta(2,4) or $\eta \sim$ Beta(4,2), the corresponding PDF and CDF of function $F(\xi, \eta)$ will be quite different, shown as Fig. 3. Since we do not know the actual distribution of $\eta$, the unfit assumption will make a large error. In this case, if we just use the bounds information, the envelope of the possible actual CDF can be obtained, i.e. the various CDF under different probability distribution are contained in the CDF belt constructed by the bounds of hybrid uncertainty (Fig. 3).

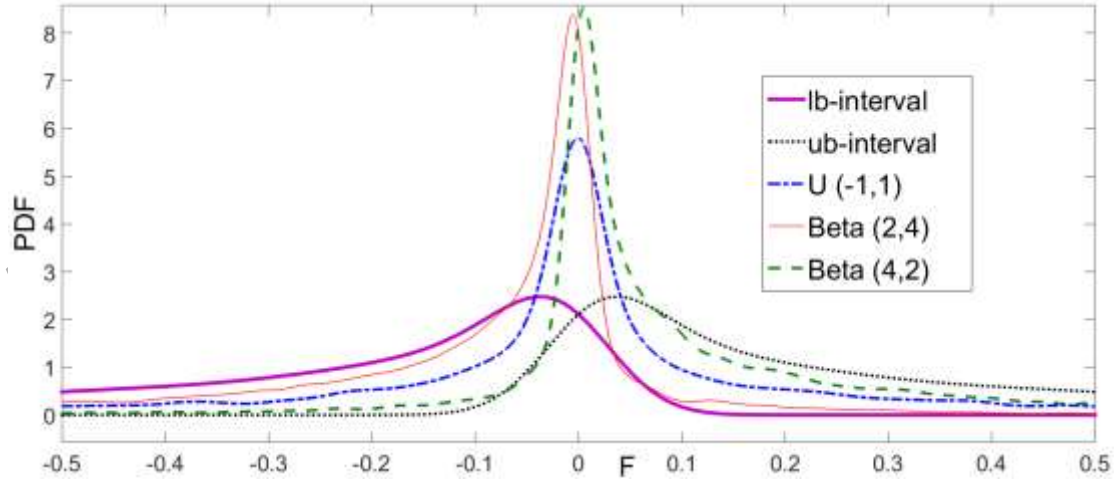


Figure 3 (a) The PDF of $F(\xi, \eta)$ for different types of random variable

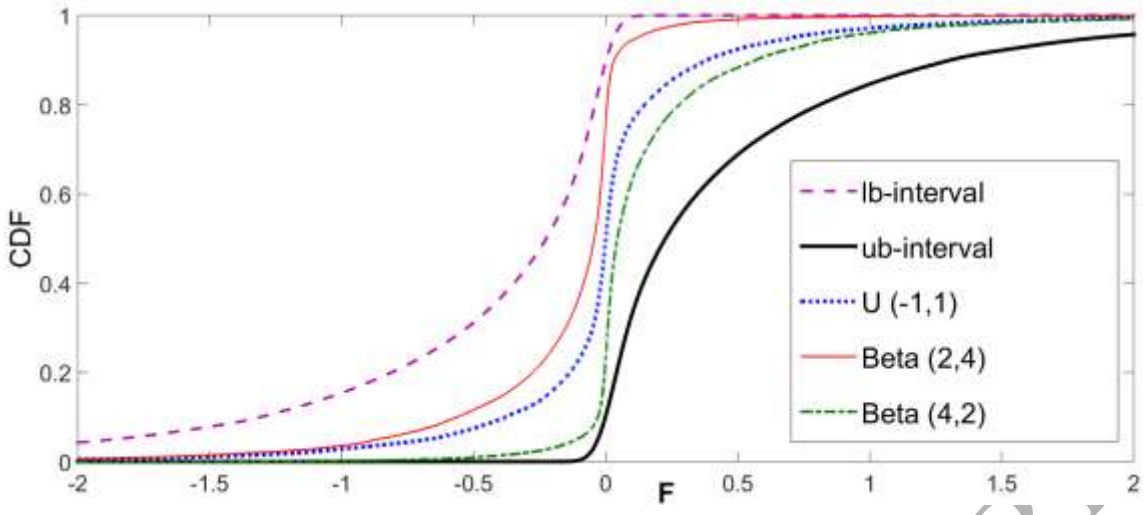


Figure 3 (b) The CDF of $F(\xi, \eta)$ for different types of random variable

## 5. Numerical examples of Structure optimization

In this section, two design optimization problems for structures that are the 18-bar planar truss and 25-bar space truss are used to show the effectiveness of the proposed design optimization method under hybrid uncertainty. The cross-section areas of the structure are the design variables, which are also considered as interval variables. The modulus of elasticity and the material density of the bar are regarded as random parameters. The results of the proposed hybrid uncertainty optimization will be compared with that of the conventional deterministic optimization and the conventional random optimization.

### 5.1 18-bar planar truss structure

Figure 4 shows the 18-bar cantilever planar truss structure. The objective function is to minimize the total weight of the planar truss by satisfying the stress limitations of ±20000lb/in$^2$ and Euler buckling compressive stress limitation:

$$b^{\sigma_i} = -\frac{KEA_i}{L_i^2}, \tag{35}$$

where $K$=4 is a constant determined by the cross-sectional geometry, $E$ is the modulus of elasticity with nominal value $10^7$ lb/in$^2$, $L_i$ is the $i$th member length, and $A_i$ denotes the cross-sectional area of the $i$th member. The minimum cross-sectional area of members is 0.1 in$^2$, and the maximum value is 50 in$^2$.

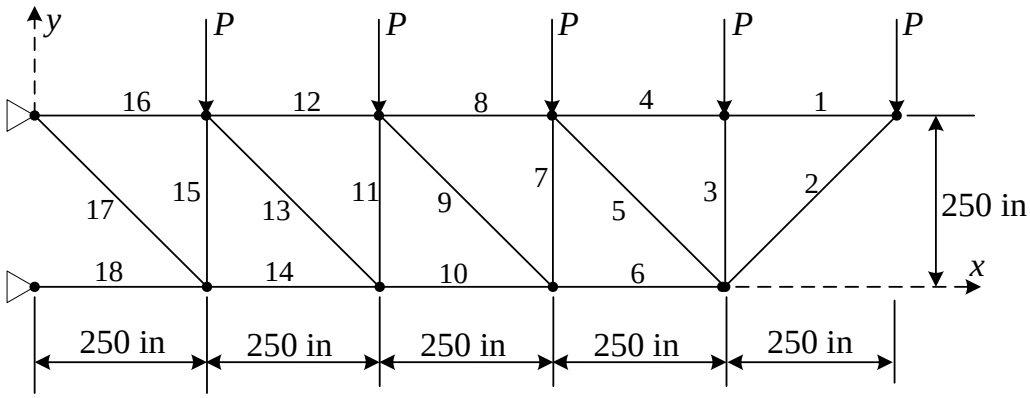


Figure 4 18-bar planar truss structure

The members can be classified into four groups when the cross-sectional areas are regarded as the design variables: $x_1$ ($A_1$, $A_4$, $A_8$, $A_{12}$, $A_{16}$), $x_2$ ($A_2$, $A_6$, $A_{10}$, $A_{14}$, $A_{18}$), $x_3$ ($A_3$, $A_7$, $A_{11}$, $A_{15}$), and $x_4$ ($A_5$, $A_9$, $A_{13}$, $A_{17}$). Considering the design variables as interval variables, the interval width is $0.1\text{in}^2$. The nominal value of the material density $\rho$=0.1lb/in$^3$, and the vertical loads is $P$=20000lb acting on the upper nodes of the planar truss. Here E and $\rho$ are considered as random parameters, satisfying the Gaussian distribution where the mean value is the nominal value and the standard deviation is 2% of the nominal value, that is $E \sim N(10^7,\ (2\times10^5)^2)$ and $\rho \sim N(0.1,\ 0.002^2)$. For this problem, the deterministic optimization formulation can be defined as follows:

$$\begin{cases} \min\limits_{\mathbf{x}} \quad f = \sum\limits_{i=1}^{18} A_i(\mathbf{x}) L_i \rho \\ \text{s.t.} \quad g_1 = \max\limits_{i=1,\ldots,18} \left(\sigma_i(\mathbf{x}) \big/ b^{\sigma_i}(\mathbf{x}, E)\right) \le 1,\ g_2 = \max\limits_{i=1,\ldots,18} \left|\sigma_i(\mathbf{x})\right| \le 20000 \\ \qquad [0.1 \quad \ldots \quad 0.1]_{1\times4}^{\mathrm{T}} \le \mathbf{x} \le [50 \quad \ldots \quad 50]_{1\times4}^{\mathrm{T}} \end{cases} \tag{36}$$

where $f$ is the total mass of the truss, $\sigma_i$ denotes the stress of the $i$th member, $g_1$ and $g_2$ are the stress constraints and Euler buckling compressive stress limitation, respectively. Three cases of the optimization will be considered:

(1) the deterministic optimization without considering uncertain parameters and variables (defined as problem (36));

(2) the uncertain optimization with considering the random parameters ($E$ and $\rho$)

$$\begin{cases} \min\limits_{\mathbf{x}} \quad f\left(\mathbf{x}, \boldsymbol{\xi}\right) \\ \text{s.t.} \quad g_1\left(\mathbf{x}, \boldsymbol{\xi}\right) \le 1,\ g_2\left(\mathbf{x}\right) \le 20000 \\ \qquad [0.1 \quad \ldots \quad 0.1]_{1\times4}^{\mathrm{T}} \le \mathbf{x} \le [50 \quad \ldots \quad 50]_{1\times4}^{\mathrm{T}} \end{cases} \tag{37}$$

where $\boldsymbol{\xi}$ denotes the random parameters $E$ and $\rho$.

(3) the uncertain optimization with considering the hybrid uncertainty for both the interval variables and random parameters

$$\begin{cases} \min\limits_{\mathbf{x}} & f\left(\mathbf{x}+[\boldsymbol{\eta}],\xi\right) \\ \text{s.t.} & g_1\left(\mathbf{x}+[\boldsymbol{\eta}],\xi\right)\le 1,\ \ g_2\left(\mathbf{x}+[\boldsymbol{\eta}]\right)\le 20000 \\ & [0.1 \quad ... \quad 0.1]^{\mathrm{T}}_{1\times 4}\le \mathbf{x}\le [50 \quad ... \quad 50]^{\mathrm{T}}_{1\times 4} \end{cases} \tag{38}$$

where the interval variables $[\boldsymbol{\eta}]=[-0.05,0.05]^4$.

The active-set algorithm in MATLAB is used to implement the optimization, with initial values of design variables $\mathbf{x}_0$=[10 10 10 10]$^{\mathrm{T}}$. The objective and constraint functions are expanded by using the 2nd order orthogonal polynomials for the hybrid uncertain optimization problem. Therefore, the collocation points will be chosen from the zeros of both the 3rd order Hermite polynomial and the Chebyshev polynomials. Since there are 2 random variables and 4 interval variables, the number of coefficients for the Hermite polynomials expansion and Chebyshev polynomials expansion will be 6 and 15, respectively. To make the least squares method stable, all the 9 zeros of the 3rd order Hermite polynomial (2 dimension) are used as the collocation points for the random variables, and 30 zeros of the 3rd order Chebyshev polynomial (4 dimension) are randomly chosen as the collocation points for the interval variables. The optimization results are shown in Table 1, which only gives the solution of the design variables. It can be found that there are only 5% difference among the three solutions. However, if we have a close look at the constraints as given in Figs. 7-9, it can be found that there are obvious differences among the three solutions. Particularly, the deterministic optimization produces the solutions which violate the constraints with higher probability, and in some cassions even more than 50%. Thus, the deterministic optimization will lead to a design that may not be feasible. The design optimization problems with uncertainties may make the optimized solution satisfy the constraints with higher probability.

Table 1 Optimization results

| | $x_1$(in$^2$) | $x_2$(in$^2$) | $x_3$(in$^2$) | $x_4$(in$^2$) |
|---|---|---|---|---|
| **Deterministic** | 10.00 | 21.65 | 12.50 | 7.07 |
| **Random** | 10.00 | 22.30 | 12.87 | 7.07 |
| **Hybrid** | 10.10 | 22.44 | 12.97 | 7.18 |

The iteration histories for the objective functions of the three optimization problems are shown as Fig. 5. It can be found that the hybrid uncertain optimization process normally converges after the first 20 iterations, so this hybrid uncertain optimization process is numerically stable.

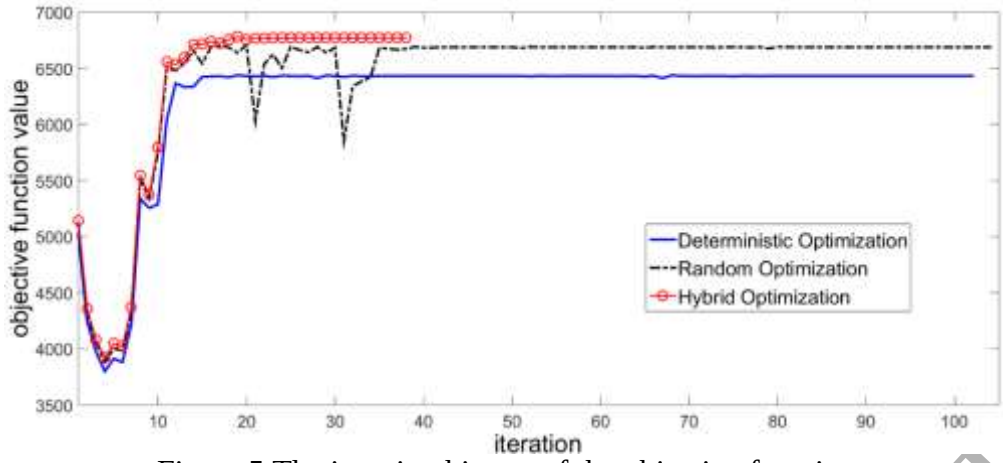


Figure 5 The iteration history of the objective function

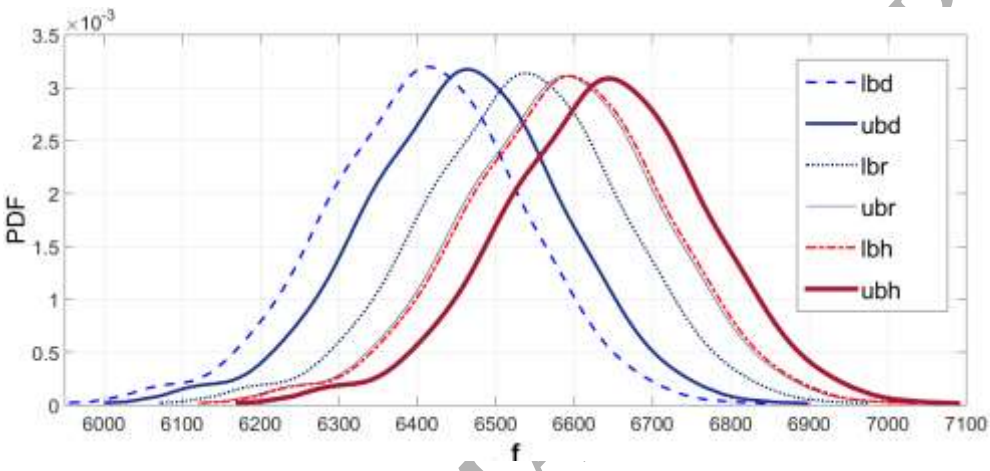


Figure 6 PDF of f

(lbd: lower bound of deterministic optimization; ubd: upper bound of deterministic optimization;
lbr: lower bound of random optimization; ubr: upper bound of random optimization;
lbh: lower bound of hybrid optimization; ubh: upper bound of hybrid optimization)

To compare the optimization results comprehensively, the PDF and CDF of the two bounds of the objective function and constraints are shown in Figs. 6-10. The constraint $g_2$ is only related to interval variables, so only its CDF is shown.

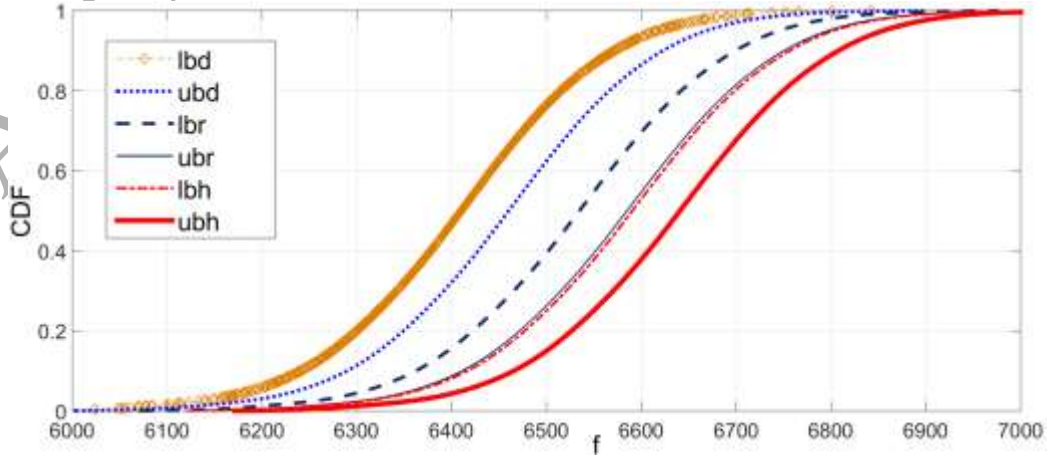


Figure 7 CDF of f

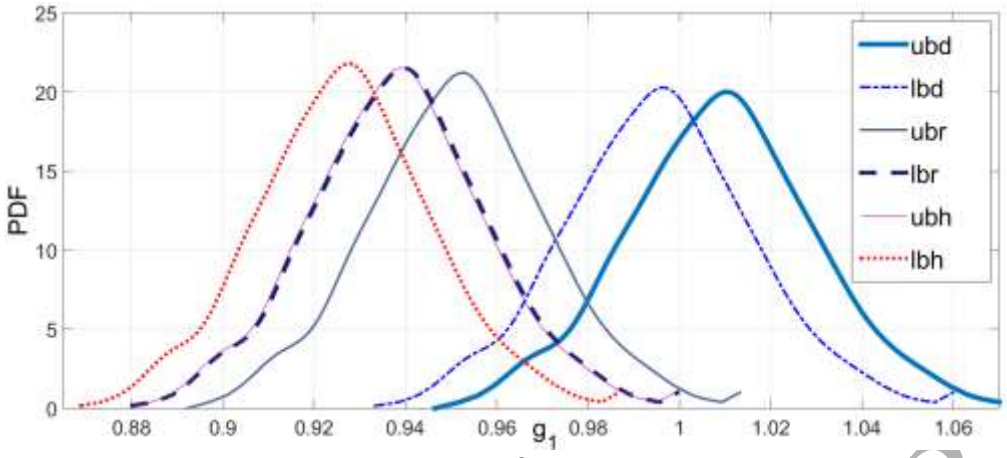


Figure 8 PDF of constraint g1

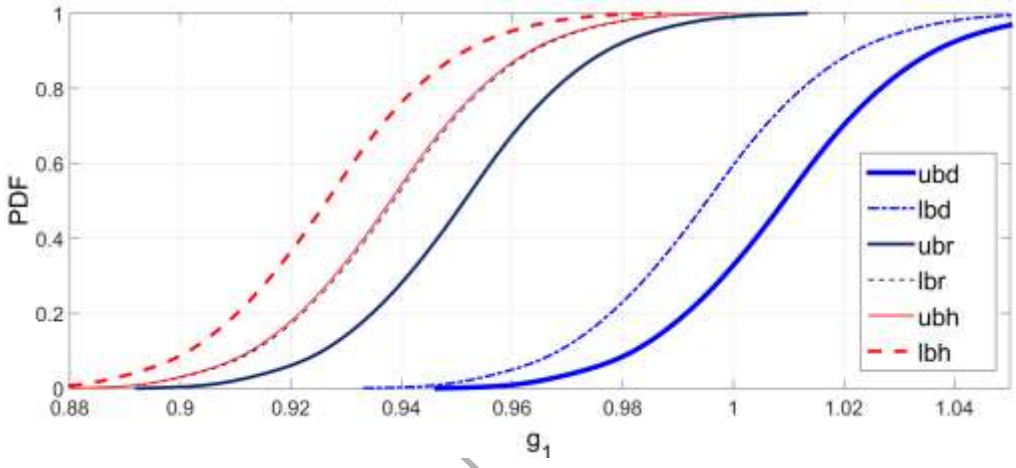


Figure. 9 CDF of constraint g1

It can be found that the objective functions of the random optimization and the hybrid uncertainty optimization are more conservative than that of the deterministic optimization. However, for the upper bound of constraint $g_1$, there are more than 60% probabilities to be violated for the deterministic optimization, while the failure probability for both the random optimization and the hybrid uncertainty optimization is very small (close to zero). The standard deviation for the solution of the hybrid optimization is smaller than the solution of the deterministic optimization, which is demonstrated by the fact that the latter has an obvious smaller peak value of PDF. However, the hybrid optimization and random optimization provide similar standard deviations, which may be induced by the following two reasons: firstly the two solutions are close; and secondly the constraint for the solutions of the different cases is weak nonlinear.

For the bounds of constraint $g_2$, the deterministic optimization and random optimization give the same results, because both of them do not consider the interval uncertainty. Therefore, the upper bounds of the deterministic optimization and random optimization are larger than the given condition (20000lb/in$^2$),

which means that the two optimization results are possible to violate the constraints. The hybrid uncertainty optimization makes the upper bound of $g_2$ smaller than 20000lb/in$^2$, which makes the optimal solution located inside the feasible region.

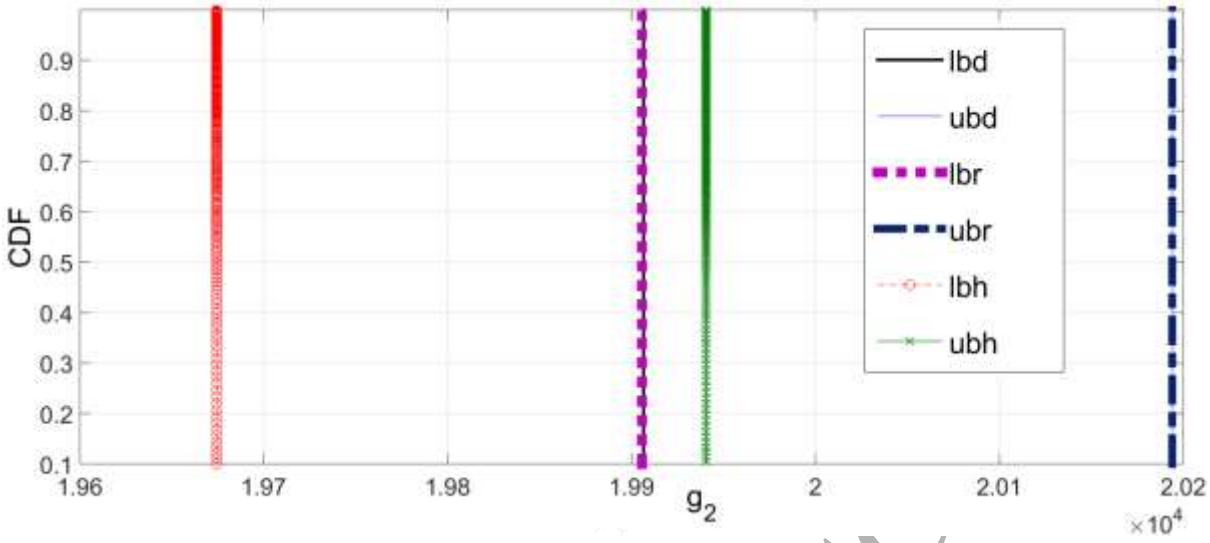


Figure 10 CDF of constraint g2

## 5.2 25-bar space truss

The 25-bar truss structure for transmission towers is shown in Fig. 11. The cross-sectional areas of truss members are regarded as interval design variables, and the interval width is 0.1in$^2$. The nominal value of the material density and the elasticity modulus is $\rho$=0.1lb/in$^3$ and E=$10^7$ lb/in$^2$, respectively, which satisfy the Gaussian distribution $E \sim N(10^7,\ (2\times10^5)^2)$ and $\rho \sim N(0.1,\ 0.002^2)$.

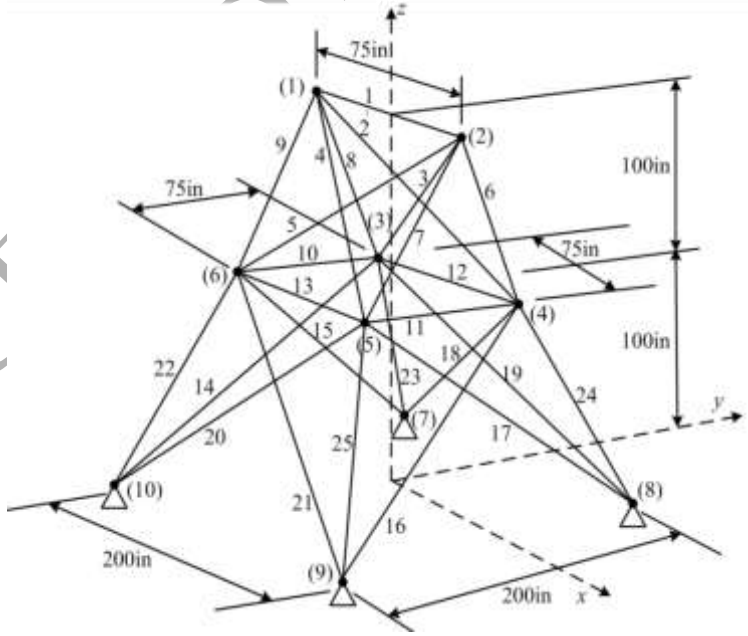


Figure 11 25-bar space truss structure

The optimization problem is to minimize the total weight of the space truss. This space truss is subjected to two loading conditions, which are shown in Table 2. The structure is required to be symmetric, so the

truss members can be grouped in Table 3, which also shows the stress limitations of each group. At the same time, the maximum displacements of nodes in each direction are limited to ±0.35in. The cross-sectional areas of all members vary in the range 0.1-10 $in^2$.

Table 2 Loading conditions

| **Node** | **Condition 1** | | | **Condition 2** | | |
|---|---|---|---|---|---|---|
| | $P_x$ (lb) | $P_y$ (lb) | $P_z$ (lb) | $P_x$ (lb) | $P_y$ (lb) | $P_z$ (lb) |
| **1** | 0 | 20000 | 5000 | 1000 | 10000 | -5000 |
| **2** | 0 | -20000 | -5000 | 0 | 10000 | -5000 |
| **3** | 0 | 0 | 0 | 500 | 0 | 0 |
| **6** | 0 | 0 | 0 | 500 | 0 | 0 |

Table 3 Member stress limitations

| **Variables** | $x_1$ | $x_2$ | $x_3$ | $x_4$ | $x_5$ | $x_6$ | $x_7$ |
|---|---|---|---|---|---|---|---|
| | $A_1$ | $A_2$ ~$A_5$ | $A_6$ ~$A_9$ | $A_{10}$ ~$A_{13}$ | $A_{14}$ ~$A_{17}$ | $A_{18}$ ~$A_{21}$ | $A_{22}$ ~$A_{25}$ |
| **Compressive stress limitations (lb/$in^2$)** | -35000 | -11000 | -17000 | -35000 | -6000 | -6000 | -11000 |
| **Tensile stress limitations (lb/$in^2$)** | 40000 | 40000 | 40000 | 40000 | 40000 | 40000 | 40000 |

The deterministic optimization formulation can be given as

$$\begin{cases} \min\limits_{\mathbf{x}} \quad f = \sum\limits_{i=1}^{25} A_i(\mathbf{x}) L_i \rho \\ \text{s.t.} \quad g_1 = \max\limits_{i=1,\ldots,25} \sigma_i(\mathbf{x}) \le 40000;\ g_2 = \min\limits_{i=1,10,\ldots,13} \sigma_i(\mathbf{x}) \ge -35000;\ g_3 = \min\limits_{i=2,\ldots,5} \sigma_i(\mathbf{x}) \ge -11000; \\ \qquad g_4 = \min\limits_{i=6,\ldots,9} \sigma_i(\mathbf{x}) \ge -17000;\ g_5 = \min\limits_{i=14,\ldots,17} \sigma_i(\mathbf{x}) \ge -6000;\ g_6 = \min\limits_{i=18,\ldots,21} \sigma_i(\mathbf{x}) \ge -6000; \\ \qquad g_7 = \min\limits_{i=22,\ldots,25} \sigma_i(\mathbf{x}) \ge -11000;\ g_8 = \max\limits_{i=1,\ldots,30} \left| d_i(\mathbf{x}, E) \right| \le 0.35; \\ \qquad \left[0.01 \quad \ldots \quad 0.01\right]_{1\times 7}^{\mathrm{T}} \le \mathbf{x} \le \left[10 \quad \ldots \quad 10\right]_{1\times 7}^{\mathrm{T}} \end{cases} \tag{39}$$

where $L_i$ is the length of the $i$th bar, $\sigma_i$ is the stress of the $i$th member, and $d_i$ represents the displacement of each node in each direction. The random optimization model and hybrid optimization model are given as follows

$$\begin{cases} \min\limits_{\mathbf{x}} & f(\mathbf{x},\boldsymbol{\xi}) \\ \text{s.t.} & g_1(\mathbf{x}) \le 40000;\ g_2(\mathbf{x}) \ge -35000; g_3(\mathbf{x}) \ge -11000;\ g_4(\mathbf{x}) \ge -17000; \\ & g_5(\mathbf{x}) \ge -6000;\ g_6(\mathbf{x}) \ge -6000; g_7(\mathbf{x}) \ge -11000;\ g_8(\mathbf{x},\boldsymbol{\xi}) \le 0.35; \\ & [0.01 \quad ... \quad 0.01]^{\mathrm{T}}_{1\times 7} \le \mathbf{x} \le [10 \quad ... \quad 10]^{\mathrm{T}}_{1\times 7} \end{cases} \tag{40}$$

$$\begin{cases} \min\limits_{\mathbf{x}} & f(\mathbf{x}+[\boldsymbol{\eta}],\boldsymbol{\xi}) \\ \text{s.t.} & g_1(\mathbf{x}+[\boldsymbol{\eta}]) \le 40000;\ g_2(\mathbf{x}+[\boldsymbol{\eta}]) \ge -35000; g_3(\mathbf{x}+[\boldsymbol{\eta}]) \ge -11000; \\ & g_4(\mathbf{x}+[\boldsymbol{\eta}]) \ge -17000; g_5(\mathbf{x}+[\boldsymbol{\eta}]) \ge -6000;\ g_6(\mathbf{x}+[\boldsymbol{\eta}]) \ge -6000; \\ & g_7(\mathbf{x}+[\boldsymbol{\eta}]) \ge -11000;\ g_8(\mathbf{x}+[\boldsymbol{\eta}],\boldsymbol{\xi}) \le 0.35; \\ & [0.1 \quad ... \quad 0.1]^{\mathrm{T}}_{1\times 7} \le \mathbf{x} \le [10 \quad ... \quad 10]^{\mathrm{T}}_{1\times 7} \end{cases} \tag{41}$$

where $\boldsymbol{\xi}$ denotes the random parameters $E$ and $\rho$, and the interval variables $[\boldsymbol{\eta}] = [-0.05, 0.05]^7$.

The initial values of the design variables are set as $\mathbf{x}_0=[1 \ \dots \ 1]^{\mathrm{T}}{}_{1x7}$. The objective and constraint functions are expanded by using the 2nd order orthogonal polynomials, with 9 collocation points of the random variables and 72 collocation points of the interval variables.

Table 4 Optimization results

| | $x_1(\mathrm{in}^2)$ | $x_2(\mathrm{in}^2)$ | $x_3(\mathrm{in}^2)$ | $x_4(\mathrm{in}^2)$ | $x_5(\mathrm{in}^2)$ | $x_6(\mathrm{in}^2)$ | $x_7(\mathrm{in}^2)$ |
|---|---|---|---|---|---|---|---|
| **Deterministic** | 0.10 | 1.77 | 2.95 | 0.10 | 0.69 | 1.95 | 2.61 |
| **Random** | 0.10 | 1.97 | 3.15 | 0.10 | 0.73 | 1.93 | 2.80 |
| **Hybrid** | 0.10 | 2.13 | 3.24 | 0.10 | 0.75 | 2.00 | 2.95 |

The optimization results are shown in Table 4, and the iteration history of the objective function is provided in Fig. 12. It can be found that the hybrid optimization model is quite stable and converges to the optimum after only 20 iterations.

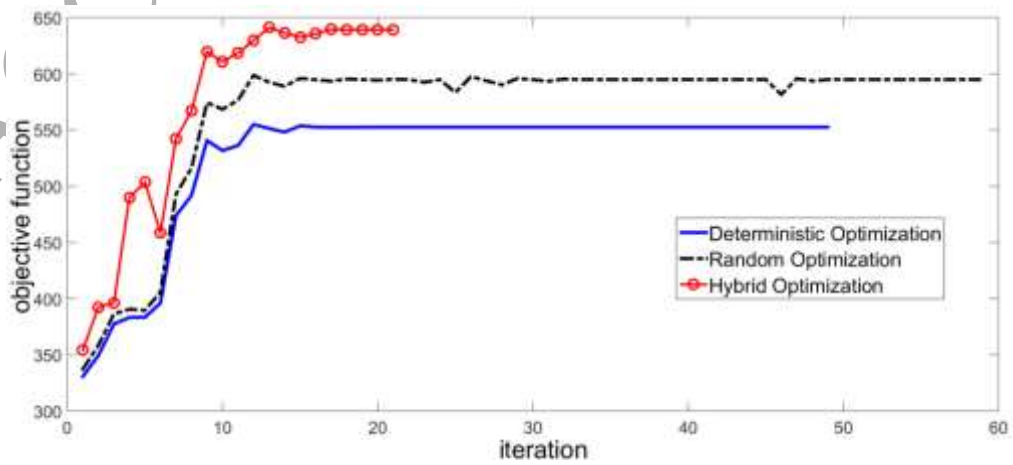


Figure 12 The iteration history of objective function

The CDF of the bounds for the objective function and active constraints are shown in Figs.13-15, respectively. The weight of the truss by using the uncertainty design optimization is larger than that of the deterministic optimization, because the constraints of the uncertainty optimization are more rigorous.

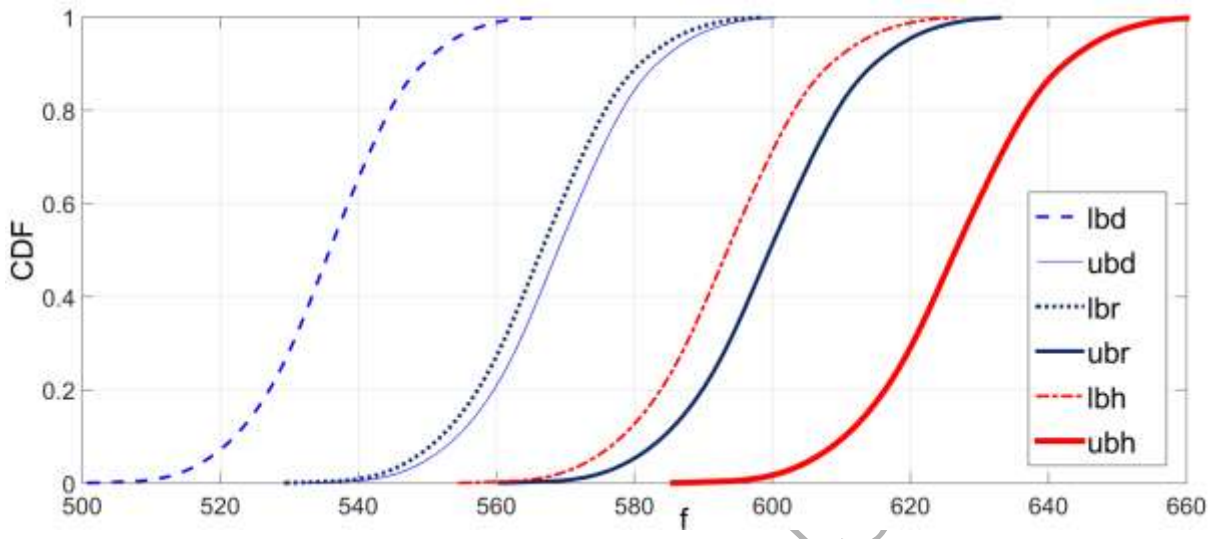


Figure 13 CDF of objective f

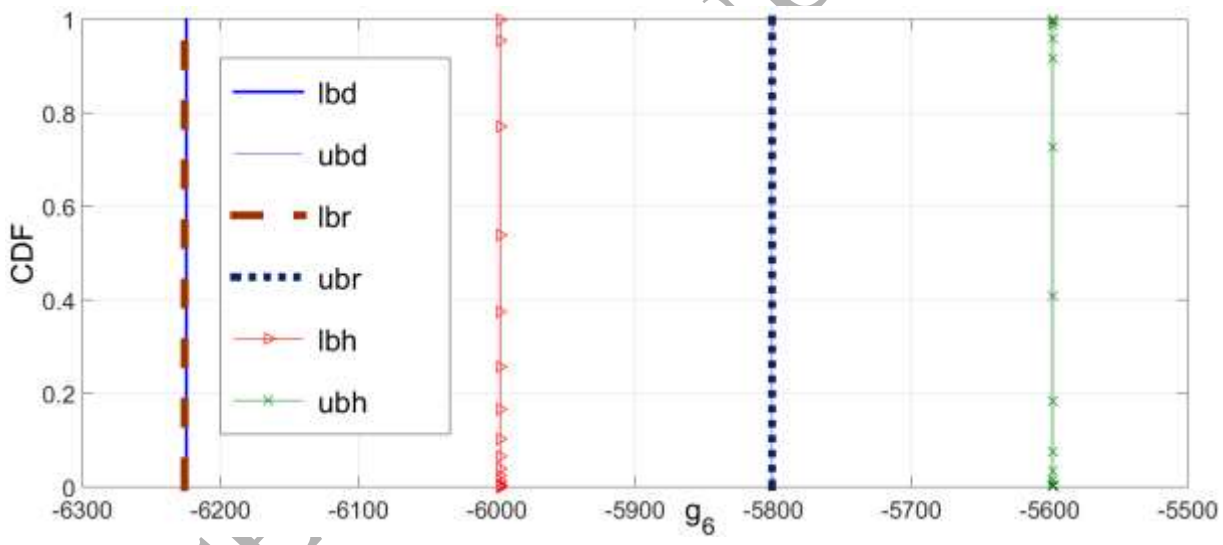


Figure 14 CDF of constraint g6

One of the active constraints $g_6$ is only related to the interval variables, so its CDF will be two vertical lines, as shown in Fig.14. Since $g_6$ is only related to the interval variables, the random optimization and the deterministic optimization almost lead to the same results, and the lower bound of $g_6$ is smaller than -6000lb/in$^2$, which indicates that the constraint is not satisfied. However, for the hybrid uncertainty design optimization, its lower bound is larger than -6000lb/in$^2$, so it satisfies the constraint even in the worst case of scenario.

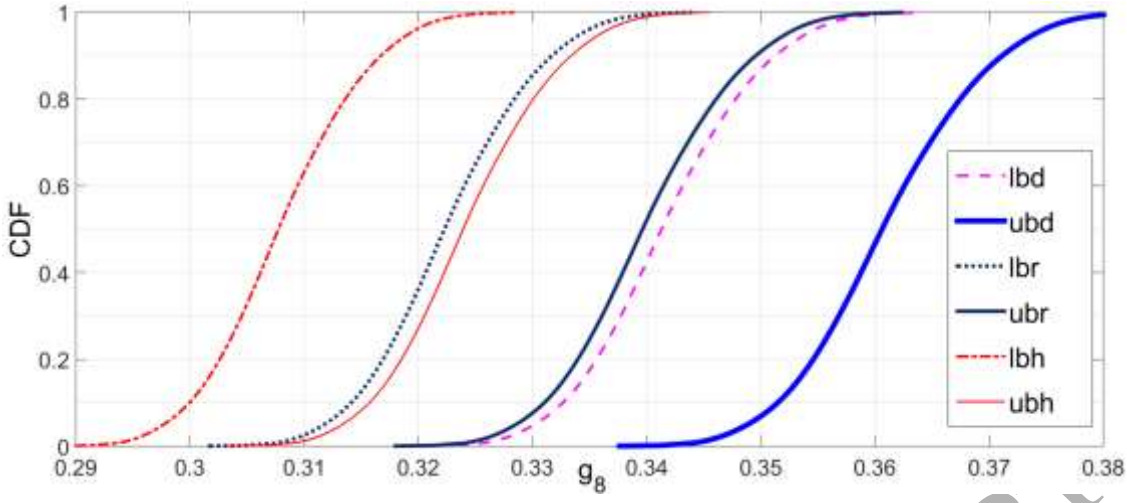


Figure 15 CDF of objective g8

The CDF of the other active constraint $g_8$ (≤0.35) are given in Figs. 15. It can be seen that the failure probability of the deterministic optimization is around 90% for the worst case of scenario. The failure probability of the random optimization is much smaller, but it is still has about 10% failure probability under the worst condition. However, the failure probability of the hybrid uncertainty optimization tends to zero under worst case of scenario.

## 6. Conclusions

This paper has developed a new hybrid uncertain design optimization method, in which both aleatory and epistemic uncertainties are considered simultaneously. The numerical analysis for the hybrid uncertainty is implemented by using the orthogonal series expansion (OSE) method. To save the computational cost, the interval arithmetic is applied to estimate the interval mean and variance of the objective and constraint functions. The design sensitivity of the objective and constraints are explicitly developed to facilitate the direct application of many gradient-based optimization algorithms. First, the results of one mathematical test example show that the proposed OSE method has similar accuracy of the Monte Carlo simulation and scanning test methods but it has much higher efficiency. Second, two typical structure optimization problems have been utilized to showcase the effectiveness of the proposed method. Their optimization results denote that the hybrid uncertainty optimization method can satisfy the constraints in the worst case, but the traditional deterministic optimization and random optimization may produce unfeasible solutions. The convengnace process demonstrates the proposed method is numerically stable and converges well.

## ACKNOWLEDGEMENTS

This research is supported by Australian Research Council (ARC) - Discovery Projects (DP150102751; DP160102491), and the National Natural-Science-Foundation of China (11502083 and 51575204), and the Science and Technology Support Program of Hubei Province of China (2015BHE026).

## References

[1] M.A. Valdebenito, G.I. Schuëller, A survey on approaches for reliability-based optimization, Structural and Multidisciplinary Optimization, 42 (2010) 645-663.
[2] Z. Kang, Y. Luo, Reliability-based structural optimization with probability and convex set hybrid models, Structural and Multidisciplinary Optimization, 42 (2009) 89-102.
[3] J. Liang, Z.P. Mourelatos, E. Nikolaidis, A Single-Loop Approach for System Reliability-Based Design Optimization, Journal of Mechanical Design, 129 (2007) 1215.
[4] A. Chiralaksanakul, S. Mahadevan, First-Order Approximation Methods in Reliability-Based Design Optimization, Journal of Mechanical Design, 127 (2005) 851.
[5] B.D. Youn, K.K. Choi, A new response surface methodology for reliability-based design optimization, Computers & Structures, 82 (2004) 241-256.
[6] M. Papadrakakis, N.D. Lagaros, Reliability-based structural optimization using neural networks and Monte Carlo simulation, Computer Methods in Applied Mechanics and Engineering, 191 (2002) 3491-3507.
[7] H.-G. Beyer, B. Sendhoff, Robust optimization – A comprehensive survey, Computer Methods in Applied Mechanics and Engineering, 196 (2007) 3190-3218.
[8] X. Du, A. Sudjianto, W. Chen, An integrated framework for optimization under uncertainty using inverse reliability strategy, Journal of Mechanical Design, 126 (2004) 562.
[9] I. Doltsinis, Z. Kang, Robust design of structures using optimization methods, Computer Methods in Applied Mechanics and Engineering, 193 (2004) 2221-2237.
[10] F. Li, Z. Luo, J. Rong, N. Zhang, Interval multi-objective optimisation of structures using adaptive Kriging approximations, Computers & Structures, 119 (2013) 68-84.
[11] X. Du, W. Chen, Sequential Optimization and Reliability Assessment Method for Efficient Probabilistic Design, Journal of Mechanical Design, 126 (2004) 225-233.
[12] T.H. Nguyen, J. Song, G.H. Paulino, Single-Loop System Reliability-Based Design Optimization Using Matrix-Based System Reliability Method: Theory and Applications, Journal of Mechanical Design, 132 (2010) 011005.
[13] J. Liang, Z.P. Mourelatos, J. Tu, A single-loop method for reliability-based design optimisation, Int. J. Product Development, 5 (2008) 76-92.
[14] J.C. Helton, J.D. Johnson, W.L. Oberkampf, C.B. Storlie, A sampling-based computational strategy for the representation of epistemic uncertainty in model predictions with evidence theory, Computer Methods in Applied Mechanics and Engineering, 196 (2007) 3980-3998.
[15] J.Y. Dantan, N. Gayton, A.J. Qureshi, M. Lemaire, A. Etienne, Tolerance Analysis Approach based on the Classification of Uncertainty (Aleatory/Epistemic), Procedia CIRP, 10 (2013) 287-293.
[16] S.K. Au, Z.-H. Wang, S.-M. Lo, Compartment fire risk analysis by advanced Monte Carlo simulation, Engineering Structures, 29 (2007) 2381-2390.
[17] G.S. Fishman, Monte Carlo: Concepts, Algorithms, and Applications., Springer-Verlag, New York, 1996.
[18] D. Xiu, G.E. Karniadakis, Modeling uncertainty in steady state diffusion problems via generalized polynomial chaos, Computer Methods in Applied Mechanics and Engineering, 191 (2002) 4927-4948.
[19] D. Xiu, G.E. Karniadakis, The Wiener-Askey polynomial chaos for stochastic differential equations, SIAM Journal on Scientific Computing, 24 (2002) 619-644.
[20] A. Gallina, Response surface methodology as a tool for analysis of uncertainty in structural dynamics, in, AGH - University of Science and Technology, 2009.
[21] W. Shi, J. Guo, S. Zeng, J. Ma, A mechanism reliability analysis method based on polynomial chaos expansion, in: 9th International Conference on Reliability, Maintainbility and Safety (ICRMS), Guiyang, China, 2011, pp. 110-115.
[22] A. Clarich, M. Marchi, E. Rigoni, R. Russo, Reliability-based design optimization applying polynomial chaos expansion: theory and applications, in: 10th World Congress on Structural and Multidisciplinary Optimization, Orlando, Florida, USA, 2013.
[23] H. Cheng, A. Sandu, Uncertainty quantification and apportionment in air quality models using the polynomial chaos method, Environmental Modelling & Software, 24 (2009) 917-925.
[24] D. Xiu, Numerical methods for stochastic computations: a spectral method approach, Princeton University Press, Princeton, 2010.
[25] E. Blanchard, A. Sandu, C. Sandu, Parameter estimation for mechanical systems via an explicit representation of uncertainty, Engineering Computations, 26 (2009) 541-569.
[26] C. Jiang, X. Han, G.P. Liu, A sequential nonlinear interval number programming method for uncertain structures, Computer Methods in Applied Mechanics and Engineering, 197 (2008) 4250-4265.

[27] S. Tangaramvong, F. Tin-Loi, D. Wu, W. Gao, Mathematical programming approaches for obtaining sharp collapse load bounds in interval limit analysis, Computers & Structures, 125 (2013) 114-126.
[28] Z. Qiu, L. Ma, X. Wang, Non-probabilistic interval analysis method for dynamic response analysis of nonlinear systems with uncertainty, Journal of Sound and Vibration, 319 (2009) 531-540.
[29] S. Chen, H. Lian, X. Yang, Interval static displacement analysis for structures with interval parameters, International Journal for Numerical Methods in Engineering, 53 (2002) 393-407.
[30] J. Wu, Y. Zhang, L. Chen, P. Chen, G. Qin, Uncertain analysis of vehicle handling using interval method, International Journal of Vehicle Design, 56 (2011) 81-105.
[31] J. Wu, Z. Luo, N. Zhang, Y. Zhang, A new interval uncertain optimization method for structures using Chebyshev surrogate models, Computers & Structures, 146 (2015) 185-196.
[32] R.E. Moore, Interval analysis, Prentice-Hall, Englewood Cliffs, New Jersey, 1966.
[33] N. Revol, K. Makino, M. Berz, Taylor models and floating-point arithmetic: proof that arithmetic operations are validated in COSY, Journal of Logic and Algebraic Programming, 64 (2005) 135-154.
[34] C.C. Li, A. Der Kiureghian, Optimal discretization of random field, Journal of Engineering Mechanics, 119 (1993) 1136-1154.
[35] J. Wu, Z. Luo, Y. Zhang, N. Zhang, L. Chen, Interval uncertain method for multibody mechanical systems using Chebyshev inclusion functions, International Journal for Numerical Methods in Engineering, 95 (2013) 608-630.
[36] J. Wang, Z. Qiu, The reliability analysis of probabilistic and interval hybrid structural system, Applied Mathematical Modelling, 34 (2010) 3648-3658.
[37] W. Gao, D. Wu, C. Song, F. Tin-Loi, X. Li, Hybrid probabilistic interval analysis of bar structures with uncertainty using a mixed perturbation Monte-Carlo method, Finite Elements in Analysis and Design, 47 (2011) 643-652.
[38] C. Jiang, W.X. Li, X. Han, L.X. Liu, P.H. Le, Structural reliability analysis based on random distributions with interval parameters, Computers & Structures, 89 (2011) 2292-2302.
[39] X. Du, A. Sudjianto, B. Huang, Reliability-Based Design With the Mixture of Random and Interval Variables, Journal of Mechanical Design, 127 (2005) 1068.
[40] K. Luo, J. Wang, X. Du, Robust mechanism synthesis with truncated dimension variables and interval clearance variables, Mechanism and Machine Theory, 57 (2012) 71-83.
[41] R. Ge, J. Chen, J. Wei, Reliability-based design of composites under the mixed uncertainties and the optimization algorithm, Acta Mechanica Solida Sinica, 21 (2008) 19-27.
[42] G.C. Marano, E. Morrone, G. Quaranta, Analysis of randomly vibrating structures under hybrid uncertainty, Engineering Structures, 31 (2009) 2677-2686.
[43] M.S. Eldred, L.P. Swiler, G. Tang, Mixed aleatory-epistemic uncertainty quantification with stochastic expansions and optimization-based interval estimation, Reliability Engineering & System Safety, 96 (2011) 1092-1113.
[44] J. Wu, Z. Luo, N. Zhang, Y. Zhang, A new uncertain analysis method and its application in vehicle dynamics, Mechanical Systems and Signal Processing, 50-51 (2015) 659-675.
[45] X. Du, P.K. Venigella, D. Liu, Robust mechanism synthesis with random and interval variables, Mechanism and Machine Theory, 44 (2009) 1321-1337.
[46] G.-J. Park, T.-H. Lee, K.H. Lee, K.-H. Hwang, Robust Design: An Overview, AIAA Journal, 44 (2006) 181-191.
[47] S. Ferson, V. Kreinovich, L. Ginzburg, K. Sentz, D.S. Myers, Constructing probability boxes and Dempster–Shafer structure, in, Sandia National Laboratories, Albuquerque, New Mexico, 2003, pp. Technical Report SAND2002-4015.